Translational Oncology 27 (2023) 101561

Contents lists available at ScienceDirect

Translational Oncology

journal homepage: www.elsevier.com/locate/tranon

Intra-tumoral infiltration of adipocyte facilitates the activation of antitumor immune response in pancreatic ductal adenocarcinoma

Xiaomeng Liu [a,b,c,d,1], Jiang Liu [a,b,c,d,1], Jin Xu [a,b,c,d,1], Bo Zhang [a,b,c,d], Miaoyan Wei [a,b,c,d], Jialin Li [a,b,c,d], Hang Xu [a,b,c,d], Xianjun Yu [a,b,c,d], Wei Wang [a,b,c,d,*], Si Shi [a,b,c,d,*]

[a] Department of Pancreatic Surgery, Fudan University Shanghai Cancer Center, Shanghai 200032, China
[b] Department of Oncology, Shanghai Medical College, Fudan University, Shanghai 200032, China
[c] Shanghai Pancreatic Cancer Institute, Shanghai 200032, China
[d] Pancreatic Cancer Institute, Fudan University, Shanghai 200032, China

ARTICLE INFO

Keywords:
Pancreatic cancer
Adipocyte infiltration
Cytokine infiltration
Antitumor immune response
Tumor microenvironment

ABSTRACT

Pancreatic ductal adenocarcinoma (PDAC) is a highly fatal malignancy that is characterized by an immunosuppressive microenvironment. The immune suppression in PDAC is largely driven by heterogeneous stromal and tumor cells. However, how adipocyte in the tumor microenvironment (TME) is related to the immune cell infiltration in PDAC has rarely been published. We identified adipocytes by performing bioinformatics analyses, and explored the clinical outcomes and TME characters in PDAC with different levels of adipocyte infiltration. Interestingly, in contrast to adiposity, high adipocyte infiltration in the TME was related to significantly increased median overall survival and a lower total tumor mutational burden. Functionally, high adipocyte infiltration was associated with the immune response, particularly with the abundant cytokine infiltration in PDAC samples. Moreover, adipocyte infiltration in the TME was positively associated with anticancer signatures in the immune microenvironment. Immunohistochemistry and RT-PCR were performed with PDAC tissue samples from our center to study the expression of adipocytes in PDAC. The mature adipocytes were strongly associated with the immune composition and prognosis of patients with PDAC. Primary adipocytes were isolated from mice to construct a PDAC transplantation tumor model. *In vivo* experiments showed that adipocytes elicited increased CD8+ T cell infiltration and potent antitumor activity in tumor-bearing mice. Overall, we innovatively found that adipocytes facilitated the antitumor immune response in the TME by performing mouse experiments and analyzing PDAC samples. This study provides a new perspective on the activation of the immune microenvironment in PDAC.

Introduction

Pancreatic ductal adenocarcinoma (PDAC) has been and remains a highly fatal malignancy with a 5-year overall survival rate of only about 7%, as approximately 80–85% of patients present either unresectable or metastatic disease due to the lack of symptoms when the cancer is still localized [1]. Only 20% of patients survive at 5 years following surgery, even patients who are diagnosed with a resectable tumor [2]. Furthermore, combination chemotherapy and radiotherapy induce only short-lived partial remission or stable disease in newly diagnosed patients [3,4]. Only <1% of patients with PDAC presenting microsatellite instability may benefit from immune checkpoint blockers (ICBs) targeting programmed death ligand-1 (PD-L1)/programmed cell death protein-1 (PD-1) [5]. Classically, PDAC exhibits an immunologically ‘‘cold’’ tumor microenvironment (TME) that is characterized by the prominent infiltration of tumor-promoting immune cells, such as myeloid-derived suppressor cells (MDSCs), and is typically devoid of CD8+ T cells [6,7]. PDAC has an abundant tumor stroma that includes a heterogeneous mixture of immune cells, endothelial cells, fibroblasts and adipocytes [8]. The immunosuppressive microenvironment of PDAC is driven by dynamic interactions between immune cells and a variety of cells and other components in host tissue [9]

* Corresponding authors at: Department of Pancreatic Surgery, Fudan University Shanghai Cancer Center, Shanghai 200032, China.
E-mail addresses: wangwei@fudanpci.org (W. Wang), shisi@fudanpci.org (S. Shi).
[1] These authors contributed equally to this work.

https://doi.org/10.1016/j.tranon.2022.101561
Received 30 May 2022; Received in revised form 6 September 2022; Accepted 3 October 2022

Obesity, especially central adiposity, is an important risk factor for the development of pancreatic cancer [10]. Excess body weight is estimated to contribute to approximately 6% (10,300 cases) of pancreatic cancer cases in men and 7% (11,200 cases) in women worldwide [11]. Regarding the systemic links between adiposity and cancer, hyperinsulinemia and insulin resistance, which are associated with an elevated cancer risk, are frequently present in obese patients with PDAC [12,13]. In addition to abnormal leptin and adiponectin levels, the obese state leads to the secretion of chemokines and inflammatory cytokines from adipose tissue [14,15]. These mediators enter the circulation and lead to systemic inflammation [16]. TME of PDAC may be influenced by systemic inflammatory factors derived from obese tissue that trigger inflammatory signaling pathways [17]. Adipose tissue adjacent to the tumor might also serve as a source of energy and growth factors not only for tumor cells but also for immune and stromal cells within the TME [18,19]. In summary, many experimental and molecular epidemiological studies have explored the relationship between excess adiposity and PDAC.

However, less research has been conducted on cancer-associated adipocytes (CAAs) in PDAC, and the role of adipocytes infiltrating the PDAC environment remains unclear. Here, we conducted a study of human samples and mouse experiments to investigate adipocyte infiltration in PDAC and to determine the role of CAAs in the patient outcomes and tumor immune microenvironment.

Results

High adipocyte infiltration predicts better outcomes of PDAC

The RNA-sequencing data of 186 patients were collected from the TCGA-PAAD dataset. A total of 142 PDAC patients with OS information remained for subsequent bioinformatic analysis after non-ductal-derived tumors were excluded. Among these patients, 129 had complete clinical information available (Table 1). A total of 167 normal samples were downloaded from the GTEx project to compensate for the insufficiency in normal tissue samples in the TCGA-PAAD dataset. Adipocytes were annotated based on gene signatures, and then a single-sample gene set enrichment analysis (ssGSEA) was conducted to estimate the adipocyte infiltration score (adipocyte IS). First, we annotated adipocytes and estimated the adipocyte IS with 21 gene signatures based on xCell. PDAC tissue had a lower adipocyte IS than normal tissue (Fig. 1A). PDAC patients were divided into two groups (high and low adipocyte IS groups) based on the median IS (Fig. 1B). We investigated whether the adipocyte IS was associated with prognosis in PDAC patients. The results showed that the median OS of patients was significantly longer in the high adipocyte IS group than in the low adipocyte IS group (Fig. 1C; P=0.0002). Next, we annotated adipocytes and estimated the adipocyte IS with 26 gene signatures based on CellMarker to verify the role of adipocytes. As expected, the adipocyte IS based on CellMarker was relatively low in PDAC (Fig. 1D). According to OS analysis, patients with a high adipocyte IS based on CellMarker showed prolonged OS compared with those with a low adipocyte IS (Fig. 1E, F; P=0.0025). In addition, we divided PDAC patients into two groups with another threshold: the high adipocyte IS (score>0) and low adipocyte IS (score<0) groups (Fig. S1A, C). The same results were found, showing that the patients in the high adipocyte IS group had a better prognosis than those in the low adipocyte IS group (Fig. S1B, D). Furthermore, immunohistochemical (IHC) staining of tumor tissue samples from patients with PDAC was performed to confirm that adipocytes commonly infiltrated the PDAC TME (Fig. 1G). For a deeper exploration of the involvement of adipocytes in PDAC progression, we isolated adipocytes from the abdominal cavity of healthy C57BL/6 mice. A low ratio of adipocytes to PDAC tumor cells was co-injected subcutaneously in C57BL/6 mice (Fig. 1H). Mice with the adipocyte co-injection showed substantial decreases in tumor growth compared to mice injected with tumor cells alone (Fig. 1I, J). Along with the analysis of samples from patients with PDAC, these results suggested that adipocytes inhibited PDAC progression.

Table 1
Characteristics of patients with PDAC in TCGA database.

Characteristics	Statistics	
	Number	%
Age		
Young	61	47
Older	68	53
Sex		
Female	61	47
Male	68	53
TNM stage		
Not reported	1	0.8
I-II	122	94.6
III-IV	6	4.6
Lymph node status		
Positive	36	28
Negative	93	72
Neoplasm histological grade		
G1	16	12
G2	76	59
G3	37	29
History of chronic pancreatitis		
Not reported	28	22
Yes	10	8
No	91	70
History of diabetes		
Not reported	23	18
Yes	28	22
No	78	60

Patients with high adipocyte infiltration have a lower tumor mutational burden (TMB)

Among the PDAC patients in the study, 122 patients with TMB data were enrolled in the following analysis. In addition, one patient whose TMB score deviated substantially from those of the other patients was excluded from this analysis. First, we calculated the total TMB of every patient and compared it between the two groups. The results showed that the patients in the high adipocyte IS group had a lower total TMB than those in the low adipocyte IS group (Fig. 2A, B). Next, we investigated the most frequent somatic mutations in the two groups. The mutation percentage refers to the percentage of samples harboring mutations in the top 20 genes among all samples. Interestingly, the mutation percentage was significantly different between the high adipocyte IS group and the low adipocyte IS group. However, the top 5 genes with somatic mutations were similar. As shown in the waterfall plot, the mutation percentage was 60% in the high adipocyte IS group. The 5 genes with the most frequent somatic mutations were TP53, KRAS, CDKN2A, TTN, and SMAD4 (Fig. 2C). In the low adipocyte IS group, the mutation percentage was 96.72%, and the 5 genes with the most frequent somatic mutations were KRAS, TP53, SMAD4, CDKN2A, and RNF43 (Fig. 2E). The co-occurrence and mutual exclusion among mutated genes were significantly different between the high adipocyte IS group and the low adipocyte IS group. In the high adipocyte IS group, co-occurrence of mutated genes was extremely common. The co-occurring mutated genes with more significant differences were the pairs TP53-KRAS, TP53-CDKN2A, TP53-TNN, KRAS-TNN, CDKN2A-ASTN1 and CDKN2A-SMAD4. Mutual exclusion was almost not observed (Fig. 2D). The TP53 and CDKN2A genes had the most co-occurring mutations in the high adipocyte IS group. Thus, as well-established highly recurrent mutations in PDAC, TP53 and CDKN2A were often accompanied by other mutations and affected the TME. CDKN2A is frequently mutated in PDAC and is known to be an important tumor suppressor gene that might synergize with TP53 to exert a tumor suppressor effect. The result suggested that the mutation of CDKN2A may cooperate with SMAD4 and ASTN1 mutations to affect tumor

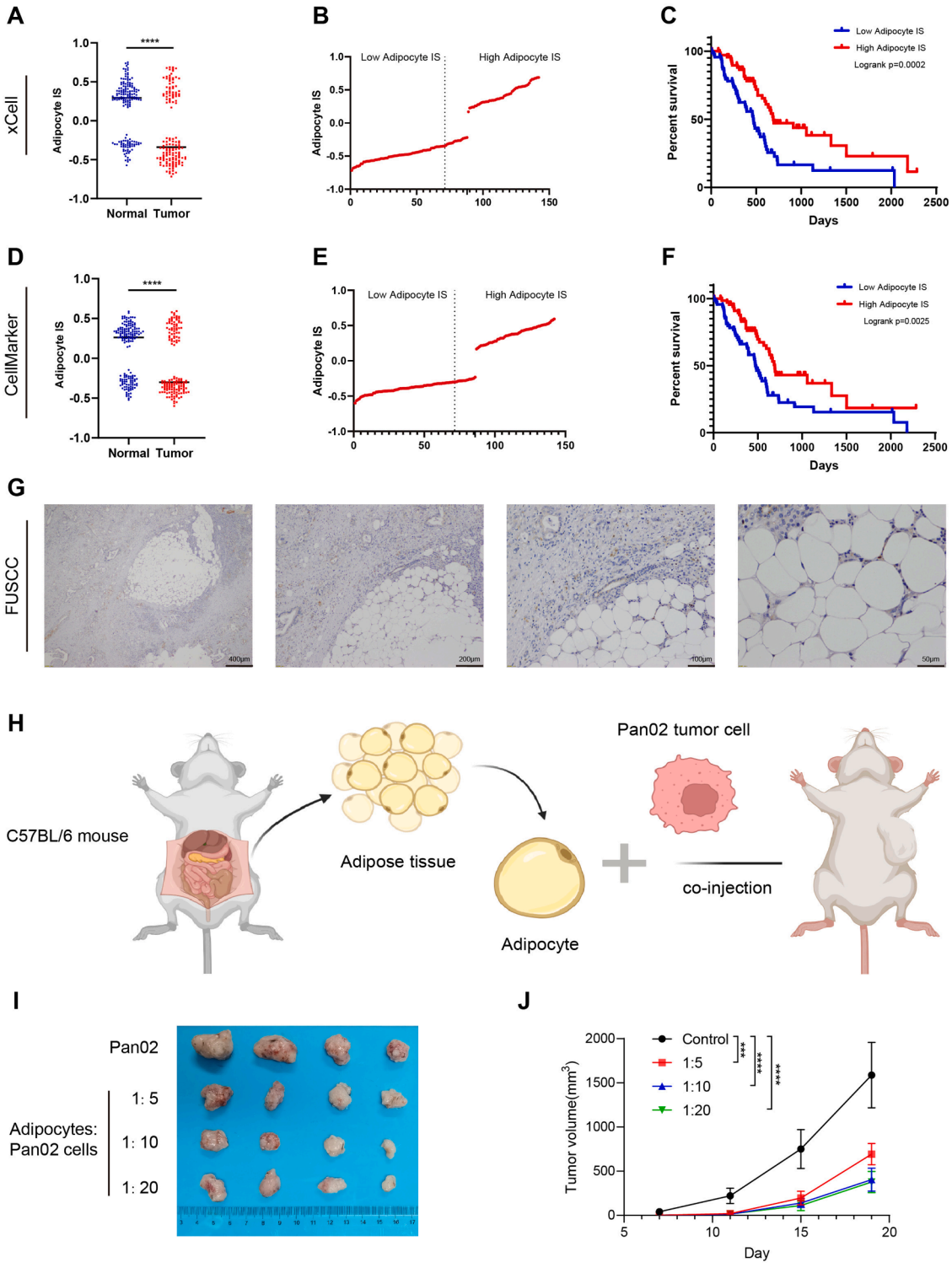

Fig. 1. Adipocyte infiltration in pancreatic tissue and the association with prognosis in PDAC. (A) Adipocyte infiltration scores (based on xCell) in normal tissue (GTEx, n=167) and PDAC tissue (TCGA, n=142). (B) PDAC patients were divided into two groups, the high adipocyte IS and low adipocyte IS groups, based on the median infiltration score (based on xCell). (C) Kaplan–Meier analysis of OS comparing the high adipocyte IS group (n=71) and low adipocyte IS group (n=71) in the TCGA (based on xCell). (D) Adipocyte infiltration scores (based on CellMarker) in normal tissue (GTEx, n=167) and PDAC tissue (TCGA, n=142). (E) PDAC patients were divided into two groups, the high adipocyte IS and low adipocyte IS groups, based on the median infiltration score (based on CellMarker). (F) Kaplan–Meier analysis of OS comparing the high adipocyte IS group (n=71) and low adipocyte IS group (n=71) in the TCGA (based on CellMarker). (G) Representative images of IHC staining for adipocytes in PDAC tissue from the FUSCC. (H) Schematic diagram depicting the construction of the mouse model transplanted with primary adipocytes and tumor cells. (I, J) Adipocytes (1×10^5 cells, 5×10^4 cells, or 1×10^4 cells) and Pan02 cells (5×10^5 cells) were co-injected subcutaneously into C57BL/6 mice. Growth curves of subcutaneous tumors were recorded (n=4 mice/group).

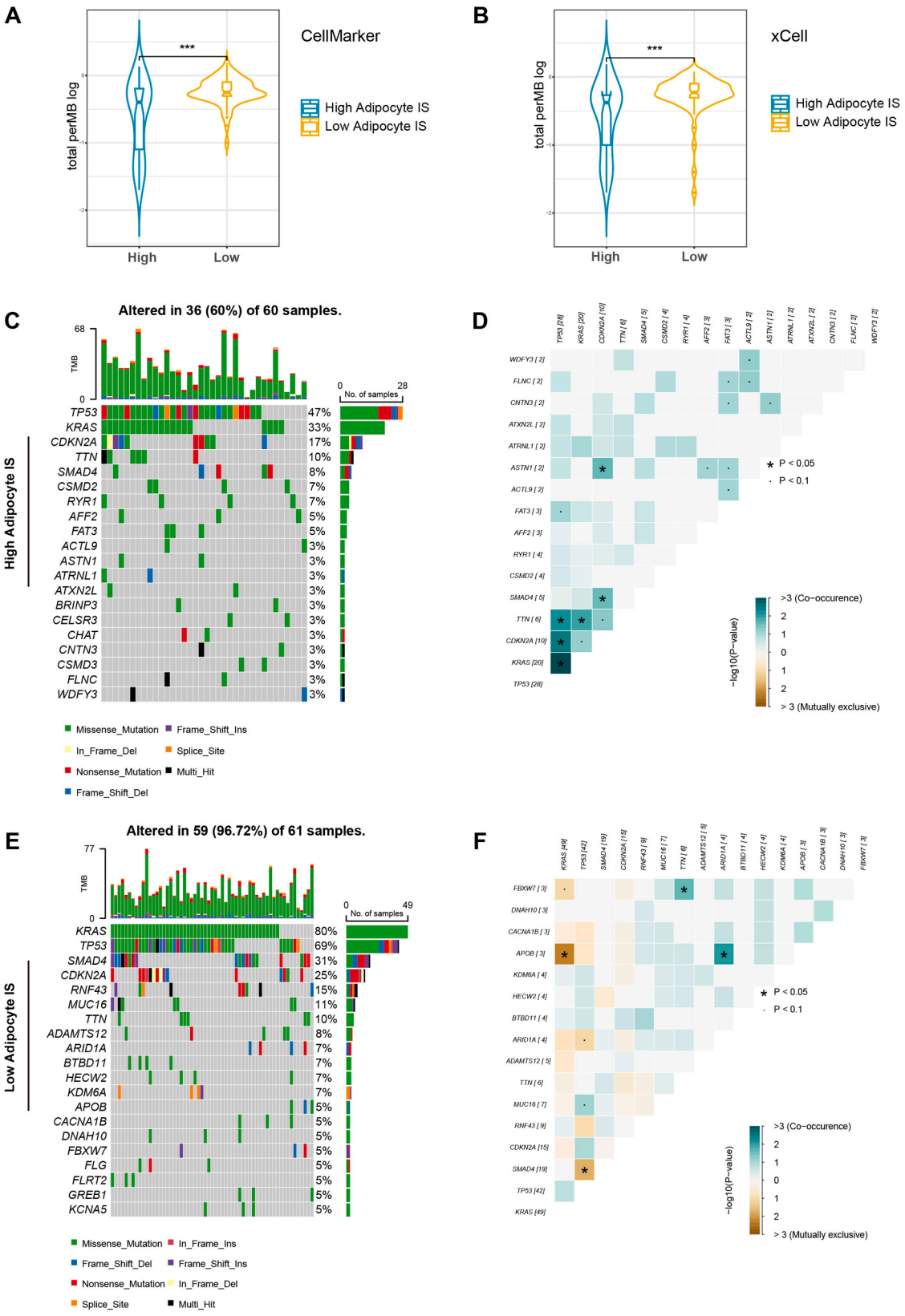

Fig. 2. Patients with high adipocyte infiltration have a lower TMB. (A, B) Violin plot of the TMB in the high adipocyte IS group (n=71) and low adipocyte IS group (n=71) in the TCGA (based on xCell and CellMarker). (C) Waterfall plot visualizing the top 20 mutated genes in the high adipocyte IS group (based on CellMarker). (D) The co-occurrence and mutual exclusion of mutated genes in the high adipocyte IS group (based on CellMarker). (E) Waterfall plot visualizing the top 20 mutated genes in the low adipocyte IS group (based on CellMarker). (F) The co-occurrence and mutual exclusion of mutated genes in the low adipocyte IS group (based on CellMarker).

progression in patients with PDAC. In contrast, the pairs KRAS-APOB and TP53-SMAD4 exhibited mutual exclusion with more significant differences. The co-occurring mutated genes with more significant differences were the pairs TNN-FBXW7 and ARID1A-APOB (Fig. 2F). In addition, the mutation percentage showed a similar significant difference when the adipocyte IS was calculated based on xCell compared with CellMarker. The mutation percentage was 93.44% in the low adipocyte IS group and 66.67% in the high adipocyte IS group (Fig. S2A, C). There were similar co-occurrence and mutual exclusion profiles for mutated genes in the two groups when xCell was used rather than CellMarker (Fig. S2B, D). In addition, TP53 and KRAS, the 2 genes with the most frequent somatic mutations, were subjected to mutation

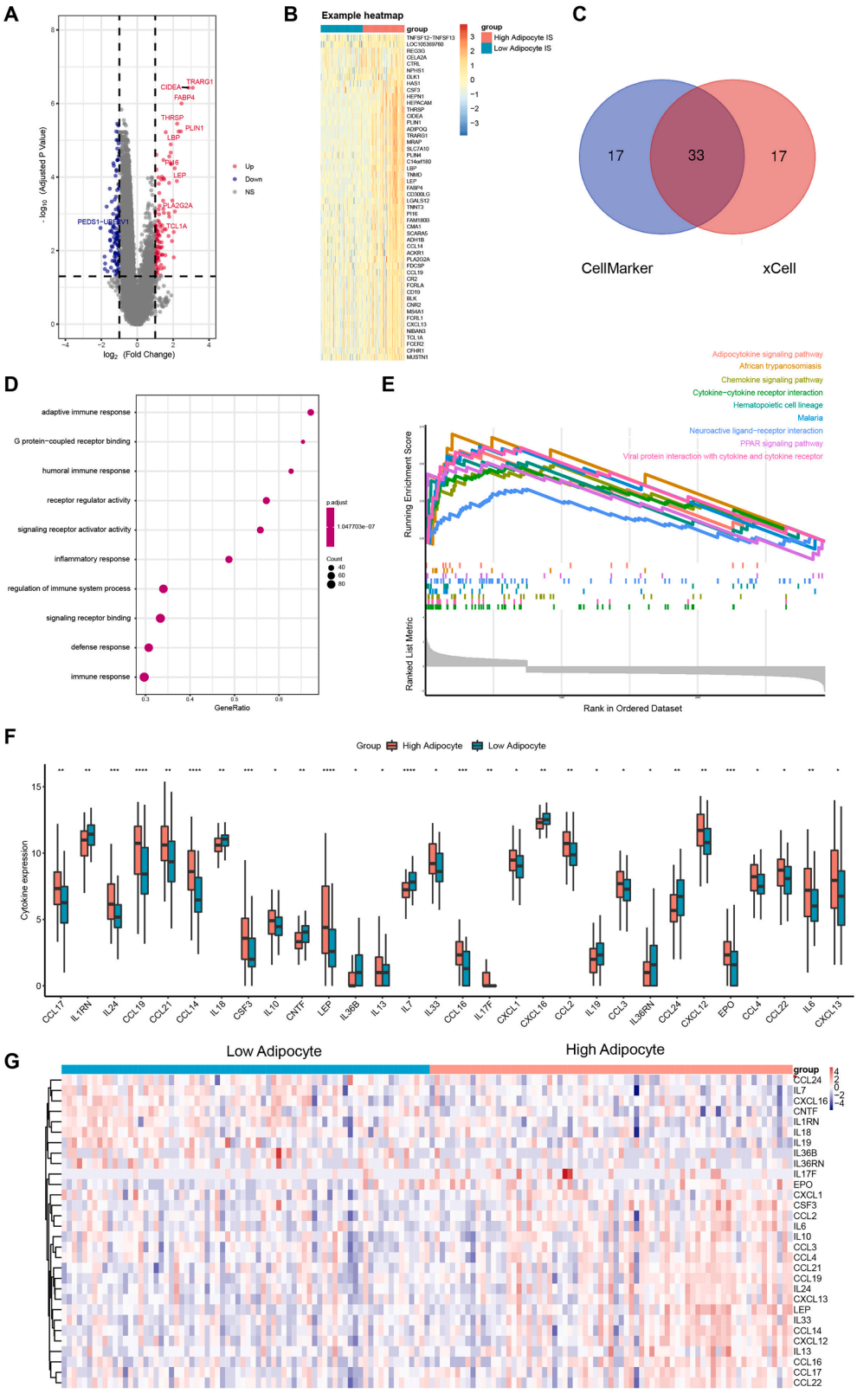

Fig. 3. High adipocyte infiltration is associated with abundant cytokine expression. (A) Volcano plot of 1591 differentially expressed genes between the high adipocyte IS group and low adipocyte IS group (LogFC > 1 and FDR < 0.05, based on CellMarker)). (B) Heatmap of the 50 most differentially expressed genes between the high adipocyte IS group and low adipocyte IS group (based on CellMarker). (C) Venn diagram of the 50 most differentially expressed genes based on xCell and CellMarker. (D) GO analysis revealing the top 10 potential functions of the differentially expressed genes. The size of round symbols refers to the counts of enriched genes. (E) GSEA showing the differentially enriched pathways of the differentially expressed genes. (F, G) Differences in the levels of 30 cytokines between the high adipocyte IS group and low adipocyte IS group.

analysis separately (Fig. S3). In summary, samples in the low adipocyte IS group had a higher total TMB and more frequent somatic mutations than samples in the high adipocyte IS group. As shown in our previous study, a low TMB predicted a better prognosis and anti-tumor immune microenvironment in PDAC [20]. The analysis of the clinical outcomes shown in Fig. 1 was consistent with the previous study, and the association between adipocytes and immune cell infiltration in PDAC will be explored next.

High adipocyte infiltration is associated with abundant cytokine expression

We identified DEGs and their potential functions in the two groups. With strict screening criteria, all DEGs were identified (Fig. 3A; Fig. S4A, B). Then, the 50 top DEGs between the high adipocyte IS group and the

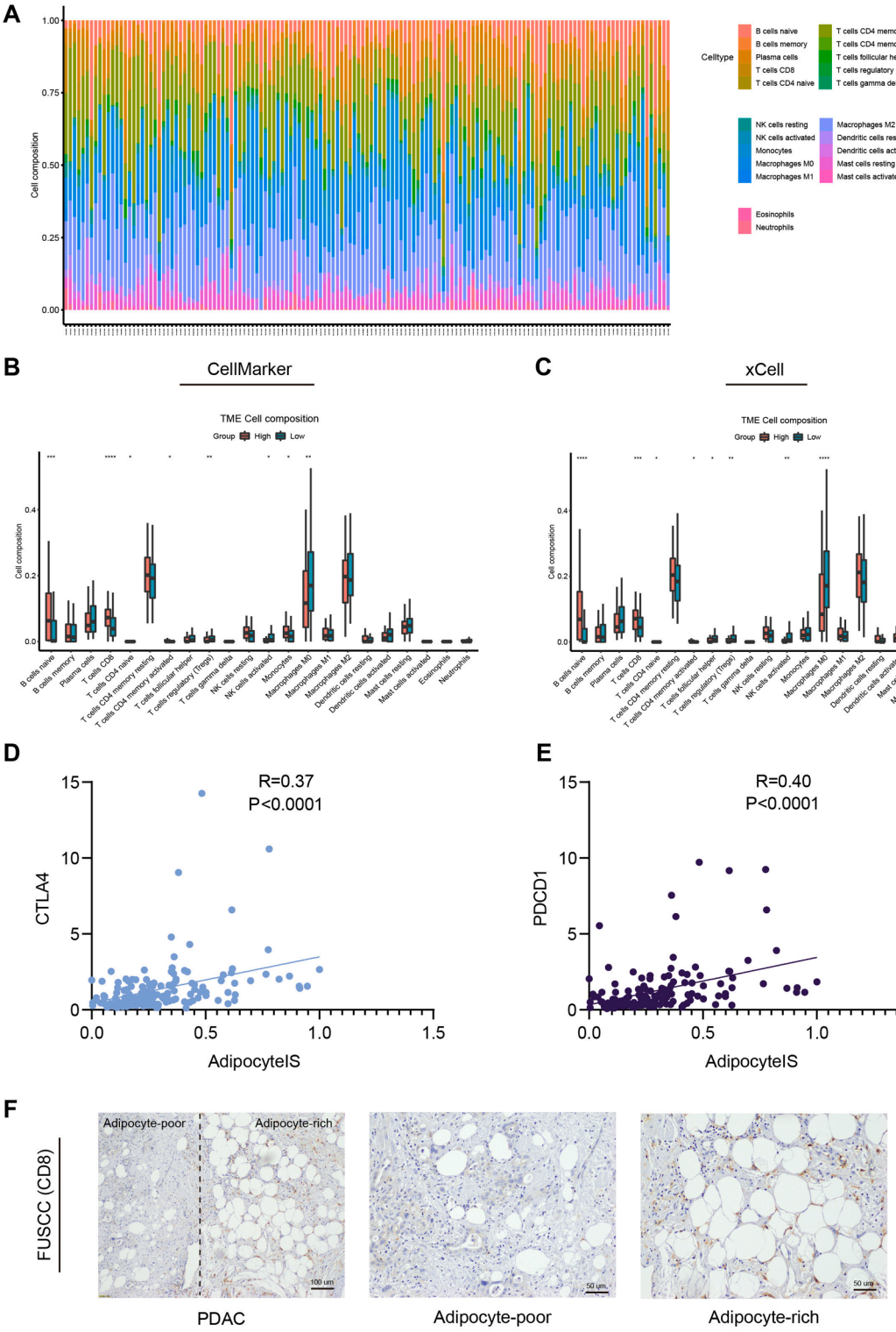

Fig. 4. The correlation between adipocyte infiltration and the immune microenvironment in PDAC. (A) Compositions of 22 immune cell types in patients from the TCGA. (B, C) Differences between the high adipocyte IS group and low adipocyte IS group in terms of the 22 immune signatures. (D, E) Correlations of the adipocyte IS with CTLA4 and PDCD1. (F) Representative images of IHC staining for CD8 in PDAC tissue from the FUSCC.

low adipocyte IS group were identified (Fig. 3B; Fig. S4C). Among the 50 top DEGs, 33 were the same between the xCell annotation analysis and CellMarker annotation analysis (Fig. 3C). Thus, these two annotation analyses of adipocytes were highly consistent and their use to define adipocytes was feasible. Gene ontology (GO) analysis revealed that the DEGs were enriched in immune response terms, such as adaptive immune response, humoral immune response and inflammatory response. In addition, we also observed that these genes might be involved in cytokine receptor-associated functions (Fig. 3D). Furthermore, GO analysis of infiltrating adipocytes based on xCell showed that the identified genes were also enriched in immune response terms, such as humoral immune response mediated by circulating immunoglobulin, immunoglobulin mediated immune response and B cell mediated immunity (Fig. S4D). Here, we showed that adipocyte infiltration might affect the immune response and regulate remodeling of the immune microenvironment in PDAC. Furthermore, we performed GSEA to identify the upregulation or downregulation of pathways in groups with differences in adipocyte infiltration. Corresponding to the GO analysis results, pathways associated with the immune response, such as the chemokine signaling pathway and cytokine−cytokine receptor interaction, were enriched in patients with PDAC presenting high adipocyte infiltration (Fig. 3E; Fig. S3E). We further analyzed the relationship between adipocyte infiltration and cytokine expression. A considerable number of cytokines showed differences in expression between the two groups (Fig. 3F). Furthermore, more abundant cytokine expression was detected in patients with PDAC presenting high adipocyte infiltration (Fig. 3G).

Adipocyte infiltration is related to anti-tumor immune microenvironment in PDAC

According to the above results, we next analyzed the association between adipocyte infiltration and immune cell infiltration in PDAC. First, we calculated the frequencies and compositions of 22 immune cell types in patients in the TCGA using the CIBERSORT algorithm (Fig. 4A). Then, we investigated the differences between the high adipocyte IS group and the low adipocyte IS group in terms of the 22 immune signatures. The most significantly different immune cells between the groups were naïve B cells and CD8+ T cells. Moreover, the results showed that these two types of immune cells were highly accumulated in the high adipocyte IS group compared with the low adipocyte IS group. In contrast, M0 macrophages and suppressive immune cells, such as regulatory T cells (Tregs), were highly accumulated in the low adipocyte IS group (Fig. 4B, C). Next, we used ssGSEA to calculate the enrichment of 29 immune signatures and further analyzed their correlations with the adipocyte IS in the TCGA database and MTAB database (Fig. S5A, B). The results showed that the adipocyte IS was positively associated with many anticancer signatures, such as those for CD8+ T cells, activated natural killer (NK) cells, T helper 1 (Th1) cells and M1 macrophages. However, the adipocyte IS was also positively correlated with M2 macrophages, a type of suppressive immune cell. Significantly positive correlations were observed between the adipocyte IS and immune checkpoints such as CTLA4 and PDCD1 (Fig. 4D, E). The positive correlation between CD274 and the adipocyte IS was not significant (Fig. S4C). Adipocyte infiltration may alter the expression of some immune checkpoints. Furthermore, IHC staining of tumor tissue from patients with PDAC revealed more CD8+ cells in the region containing infiltrating adipocytes than in the other stromal regions in PDAC tissues (Fig. 4F). Overall, the adipocyte IS was associated with immune cell compositions in the TME, despite slight differences in the results generated with different algorithms. Generally, adipocyte infiltration was positively associated with anticancer signatures in the immune microenvironment.

Adipocyte infiltration is associated with prognosis and the immune microenvironment in PDAC patients

FABP4, which is expressed in only mature adipocytes, was detected in PDAC tissue samples from the Fudan University Shanghai Cancer Center (FUSCC) to validate the results from the bioinformatics analysis (Table 2). The RT-PCR analysis of tissues from the FUSCC showed that FABP4 was expressed at high levels in adjacent tissues compared with tumor tissues (Fig. 5A). Next, we sought to determine whether FABP4 affects the survival of PDAC patients. The data from our center showed that FABP4 expression was positively correlated with the median OS of patients (Fig. 5B). Furthermore, analysis of data from the TCGA validated the positive correlation between prognosis and FABP4 (Fig. 5C). Additionally, we explored the relationship between FABP4 and the immune composition in the PDAC TME. Interestingly, FABP4 expression was strongly positively correlated with CD8+ T cell infiltration in PDAC ($r = 0.453$, $P < 0.001$) compared with other tumors (Fig. 5D, E). In addition, FABP4 had a strong negative association with myeloid-derived suppressor cell (MDSC) infiltration in PDAC (r=−0.497, $P < 0.001$) in contrast with other tumors (Fig. 5D, F). These results suggested that FABP4 might have a more significant role in PDAC than in other tumors. IHC staining of tissues from the FUSCC indicated that FABP4 was commonly expressed in adipocytes in PDAC samples. There were also many CD8+ T cells among the cells highly expressing FABP4 (Fig. 5G). Overall, FABP4 was commonly expressed in adipocytes in the PDAC TME. FABP4 expression was positively associated with CD8+ T cells and negatively associated with MDSCs in PDAC. These associations are a possible reason that FABP4 was positively correlated with a better prognosis.

RT-PCR was used to detect the expression of 21 genes that defined adipocytes based on the xCell algorithm in tumor tissues from FUSCC as a method to better validate the role of adipocytes in PDAC. Then ssGSEA was conducted to estimate adipocyte infiltration in PDAC, and patients were divided into two groups based on the level of adipocyte infiltration (Fig. 6A). Next, data from our center showed that adipocyte infiltration was positively correlated with the median OS of PDAC patients (Fig. 6B). IHC staining of corresponding tumor tissues from FUSCC used in the ssGSEA analysis showed that more CD8+ T cells were present in PDAC with high adipocyte infiltration (Fig. 6C). This result is consistent with the bioinformatics analysis shown in Fig. 4. We detected the expression of cytokines that showed significant differences in Fig. 3 to explore the relationship between cytokine infiltration and adipocyte infiltration in

Table 2
Characteristics of patients with PDAC treated at the FUSCC.

Characteristics	Statistics	
	Number	%
Age		
>60 years	31	44
≤60 years	39	56
Sex		
Female	30	43
Male	40	57
TNM stage		
I-IIa	38	54
IIb-IV	32	46
Tumor size		
≥4.0 cm	18	26
<4.0 cm	52	74
Histological grade		
Low	31	44
High/moderate	39	56
Lymph node status		
Positive	37	53
Negative	33	47
CA19-9 ≥ 37 U/mL		
Yes	61	87
No	9	13

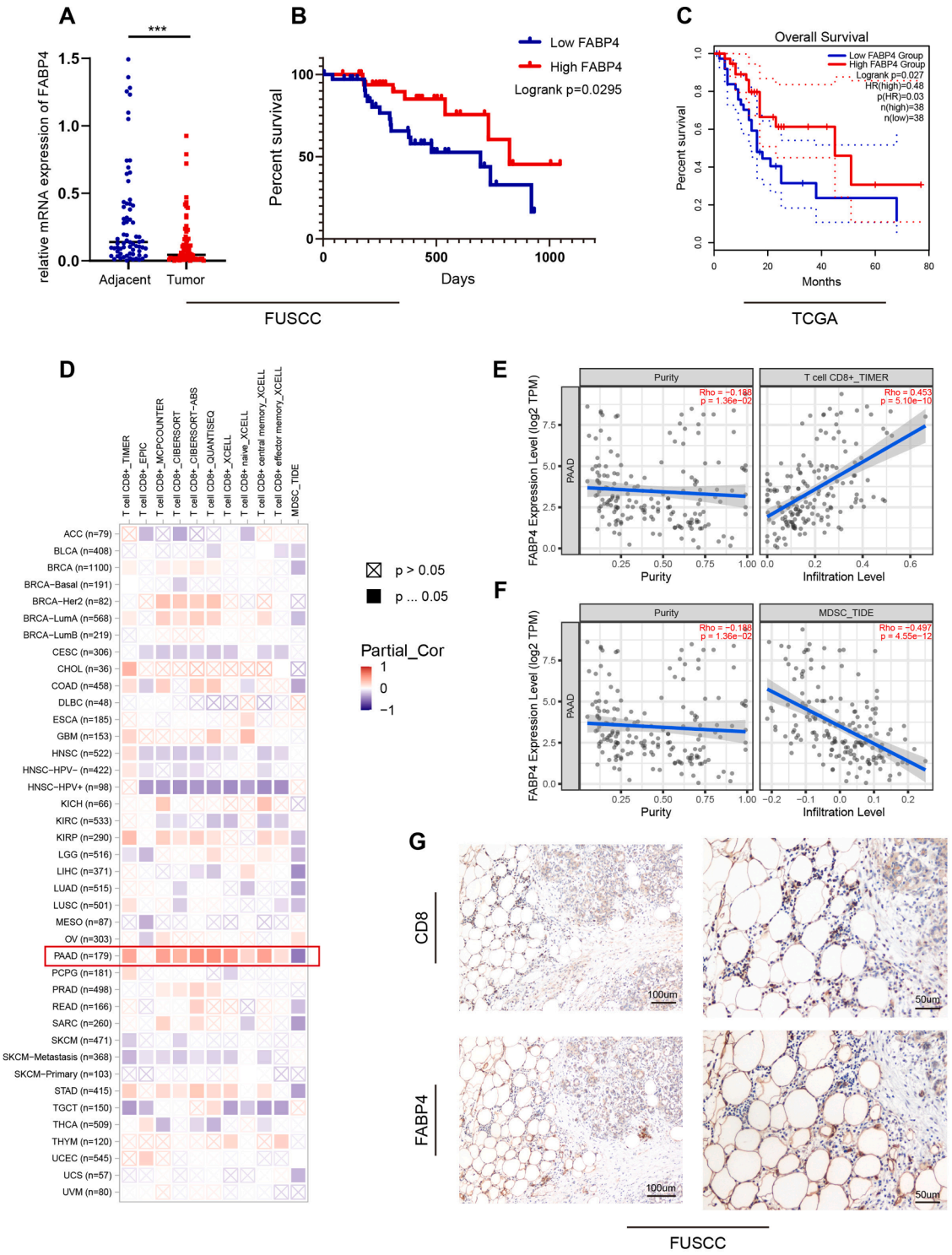

Fig. 5. FABP4 is associated with prognosis and the immune microenvironment in PDAC. (A) mRNA expression of FABP4 in 68 paired PDAC tissues (adjacent tumor tissue and tumor tissue) from the FUSCC. (B) Kaplan–Meier analysis of OS comparing samples in the high FABP4 group (n=35) and those in the low FABP4 group (n=35) from the FUSCC. (C) Kaplan–Meier analysis of OS comparing the high FABP4 group (n=38) and low FABP4 group (n=38) from the TCGA. (D) Correlations of FABP4 and CD8+ T cells or MDSCs in tumors. (E) FABP4 expression was positively associated with CD8+ T cells in PDAC based on the TCGA dataset. (F) FABP4 expression was negatively associated with MDSCs in PDAC based on the TCGA dataset. (G) Representative images of IHC staining for FABP4 and CD8 in PDAC tissues from the FUSCC.

tumor tissues from patients treated at FUSCC. The results also showed more abundant cytokines, especially chemokines, in tumor tissues with high adipocyte infiltration (Fig. 6D). Chemokines are best known for their roles in recruiting immune cells into the TME, and exert distinct effects on tumor progression [21]. Different immune cell subsets are recruited into the TME by different chemokines, and the specific chemokine population ratio determines the abundance of anticancer immune cells in PDAC with high adipocyte infiltration. However, further studies are needed to explore whether these cytokines play roles in immune checkpoint activation.

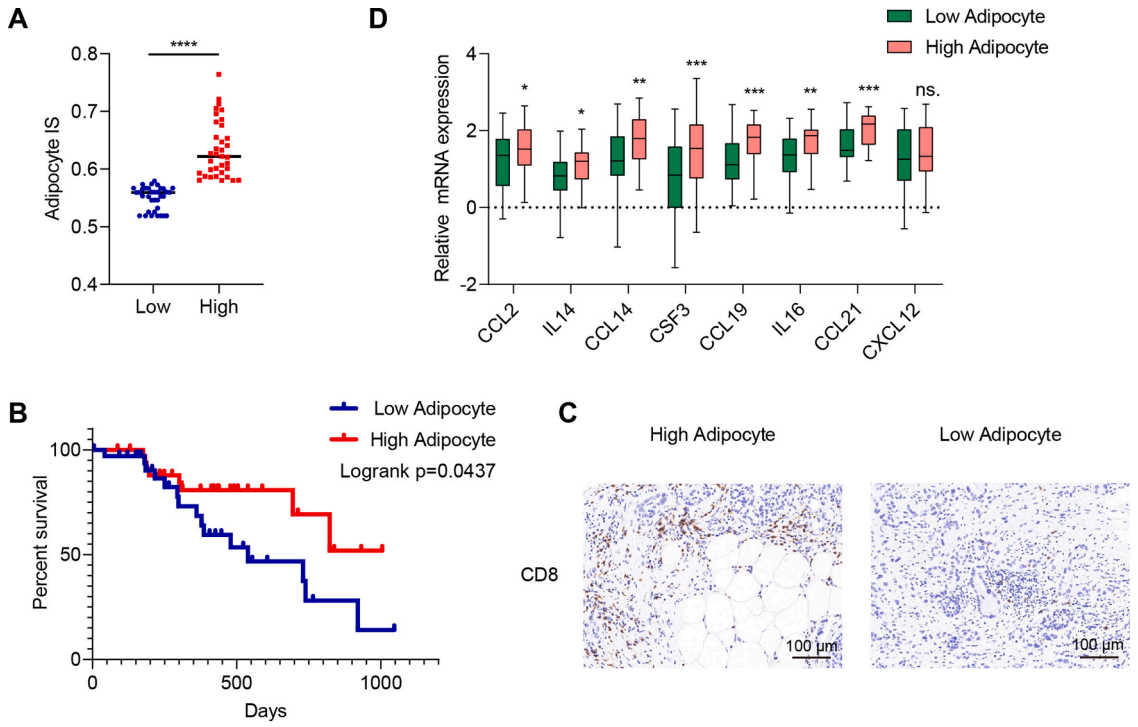

Fig. 6. Adipocyte infiltration is associated with prognosis and the immune microenvironment in PDAC. (A) Adipocyte infiltration scores for PDAC tissues from the FUSCC (n=70). (B) Kaplan–Meier analysis of OS comparing samples in the high adipocyte infiltration group (n=35) and those in the low adipocyte infiltration group (n=35) from the FUSCC. (C) Representative images of IHC staining for CD8 in PDAC tissues from the FUSCC. (D) Differences in the expression of cytokines in PDAC samples from the FUSCC with different levels adipocyte infiltration.

Adipocytes elicit increased antitumor immune cell infiltration in tumor-bearing mice

We performed a flow cytometry analysis of tumor-infiltrating immune cells collected from subcutaneous tumor tissue samples from C57BL/6 mice to further investigate the role of adipocytes in immune cell infiltration into PDAC. A substantial increase in the number of CD3+ CD8+ T cells was observed in mouse tumor tissues co-injected with adipocytes compared to mice injected with tumor cells alone (Fig. 7A, C). Consistent with the flow cytometry analysis, IHC staining showed the same increase in the number of CD8+ T cells in mouse tumor tissues co-injected with adipocytes (Fig. 7B, D). These results indicated the involvement of adipocytes in antitumor immune cell infiltration in tumor-bearing mice.

Overall, we found that adipocyte infiltration in the TME facilitated abundant cytokine infiltration and was positively associated with anti-cancer immune signatures in PDAC according to the bioinformatics analysis and *in vitro* experiments (Fig. 8). Our results provide a new perspective on the activation of the immune microenvironment in PDAC.

Discussion

Epidemiological evidence implicates obesity as a risk factor for the development of pancreatic cancer [22]. Additionally, a higher pre-diagnosis BMI is associated with shorter survival among patients with pancreatic cancer [23]. However, a relationship has not been observed between BMI after diagnosis and the survival of patients with pancreatic cancer, and research on the role of infiltrating adipocytes in PDAC progression has not been conducted. In the present study, we detected a lower number of adipocytes infiltrating the tumor than the normal tissue, and this value was positively associated with the prognosis. In contrast to obesity, adipocytes infiltrating the TME seem to be a protective factor for patients with PDAC. An intensely desmoplastic stroma is one of the hallmarks of PDAC, and it may limit the infiltration of adipocytes to some extent [24]. Given the relatively low proportion of adipocytes infiltrating the PDAC tumor tissue, a lower ratio of adipocytes to tumor cells was co-injected in the mouse PDAC transplantation model. The limited number of adipocytes exerted an antitumor effect on tumor growth in the mouse PDAC model. However, additional studies are needed to elucidate whether adipocytes that are actively infiltrating play the same role in tumor development.

Mutations in KRAS were first associated with PDAC and were supported by genetically engineered mouse models of the disease [25]. KRAS mutation is necessary but not sufficient for PDAC development. Many additional mutations, such as TP53, SMAD4 and CDKN2A mutations, and environmental conditions, including obesity and inflammation, markedly accelerate PDAC development in mouse models. However, KRAS activity was not significantly different between pancreas samples from obese and lean mice [26]. According to our bioinformatics analysis, patients with low adipocyte infiltration have higher somatic mutation frequencies. In the low adipocyte IS group, the 5 genes with most frequent somatic mutations were KRAS, TP53, SMAD4, CDKN2A, and RNF43. In the high adipocyte IS group, the 5 genes with most frequent somatic mutations were TP53, KRAS, CDKN2A, TTN, and SMAD4. Apparently, genes with mutations in the low adipocyte IS group were more consistent with common gene mutations in PDAC. Mutations in these genes might influence adipocyte infiltration in the TME by regulating cytokine and chemokine production. An overall high mutational burden may be detrimental to adipocyte infiltration, and these co-mutated genes may exert similar or synergistic effects on adipocyte infiltration. However, this study of the mutation burden has limitations. PDAC is characterized by an abundant tumor stroma and the cells with a non-cancerous genome may impact the TMB estimate [27]. The mutation burden of PDAC might be affected by intra-tumoral infiltrating adipocytes, and thus the correlation with the TMB may be partially biased by the tumor specimen.

Obesity alters circulating factors associated with a systemic

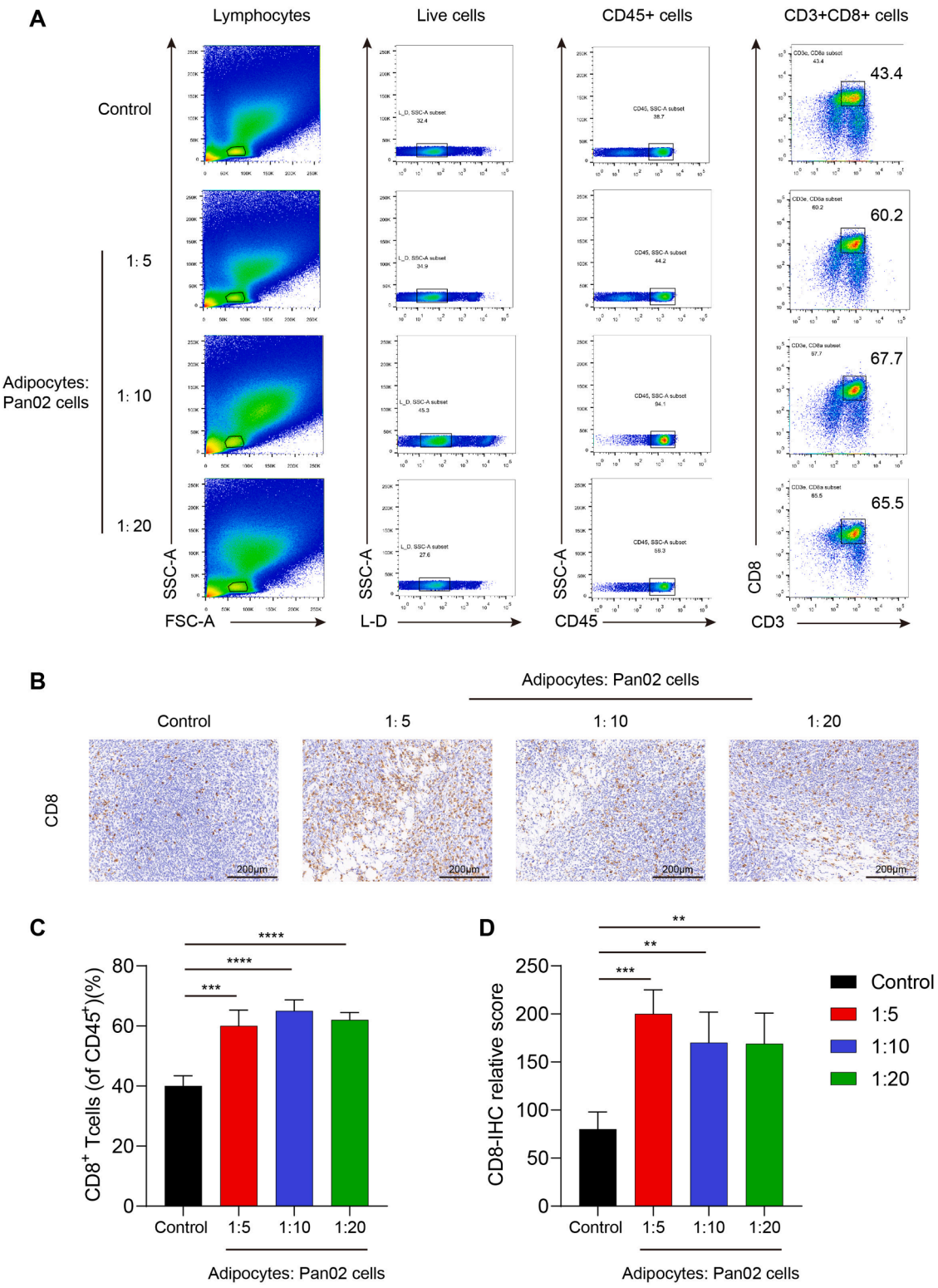

Fig. 7. Adipocytes elicit increased antitumor immune infiltration in tumor-bearing mice. (A, C) Numbers of CD3+CD8+ T cells in subcutaneous tumors from each group were measured using flow cytometry. (B, D) Representative images and quantification of IHC staining for CD8 in tumor tissues from each group of mice. Scale bar, 200 μm.

inflammatory state, including leptin, IL-6, IFNγ, TNF, growth factors and a range of chemokines [28,29]. These alterations induce changes in the frequencies of circulating immune cells, including decreased numbers of activated CD8+ cytotoxic T lymphocytes and Treg cells and increased numbers of M1-type macrophages, CD4+ T cells, B cells and NK cells [30,31]. However, changes in circulating immune cells appear to depend on the extent of obesity. In this study, pathways associated with the immune response, such as the chemokine signaling pathway and cytokine–cytokine receptor interaction, were enriched in patients with PDAC presenting high adipocyte infiltration. PDAC is an immunologically "cold" tumor with few immune cells [32]. Adipocyte-induced chemokine and cytokine production may help change this situation.

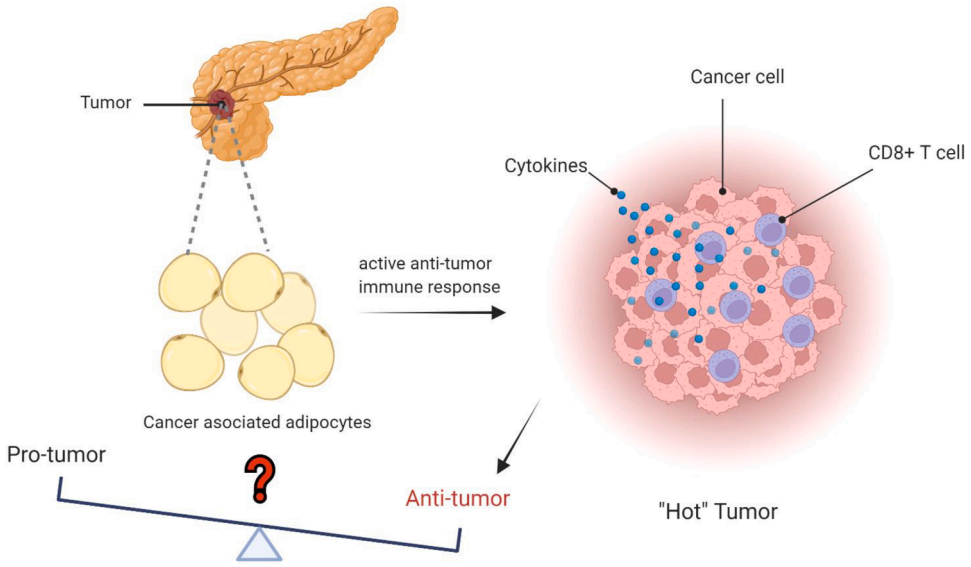

Fig. 8. Intra-tumoral adipocytes induce an antitumor immune response in PDAC.

Adipocyte infiltration is positively associated with anticancer signatures in the immune microenvironment, such as CD8+ T cells and activated NK cells. FABP4, which is expressed only in mature adipocytes, was detected in PDAC tissues. FABP4 was positively correlated with CD8+ T cells and negatively correlated with MDSCs both in TCGA database and tumor tissues from the FUSCC. Additionally, high FABP4 expression predicted a better prognosis. However, this study had limitation, the inhomogeneity of specimens produced some discrepancies. Because of the limitation of experimental conditions, we only detected FABP4 expression in tumor tissue but not the expression of a cluster of signature genes. This study is simply a correlation study, the mechanism underlying the role of adipocyte infiltrating in the TME requires more exploration.

In conclusion, according to the bioinformatics analysis and *in vitro* experiments, we found the high adipocyte IS in the TME predicted a significantly longer median overall survival. Samples with low adipocyte infiltration had a higher TMB and more frequent somatic mutations. Differentially expressed genes were functionally enriched in pathways associated with the immune response. Adipocyte infiltration in the TME was positively associated with anticancer immune signatures. Overall, we innovatively explored the function of adipocytes infiltrating the TME by performing bioinformatics analyses, *in vitro* experiments, and mouse experiments. Our results provide a new perspective on the role of CAAs in PDAC.

Materials and methods

Data sources and selection

RNA-sequencing data were collected from The Cancer Genome Atlas (TCGA)-pancreatic adenocarcinoma (PAAD) dataset [33]. According to the annotations of TCGA-PAAD, we excluded non-ductal-derived tumors and normal adjacent samples. Only PDAC samples remained for subsequent bioinformatic analysis. Normal samples were collected from the Genotype-Tissue Expression (GTEx) project to compensate for the insufficiency of normal tissues in TCGA-PAAD dataset. Clinical data such as overall survival (OS) were also downloaded from the abovementioned datasets.

Estimation of the intra-tumoral infiltrated adipocyte score

An ssGSEA analysis was conducted to calculated the expression levels of intratumoral infiltrated adipocytes using the Gene Set Variation Analysis (GSVA) package (v1.30.0) [34] ssGSEA enrichment scores were calculated using gene sets comprised of genes characteristic of adipocyte infiltration signatures. Adipocyte infiltration was annotated with xCell, a bioinformatics algorithm that defined adipocytes based on the expression pattern of 21 genes, as reported by Aran et al. [35]. Then, the results were validated and corrected with the CellMarker database, a manually curated resource of cell markers in human and mouse [36]. Each sample was labeled with an enrichment score for the specific hallmark gene signature. The samples were divided into two groups (high adipocyte IS and low adipocyte IS) based on the median infiltration score and were visualized in a scatter plot. The difference in survival between two groups was assessed by plotting Kaplan-Meier curves. The log rank test was performed to verify the statistical significance of the difference in survival. $P < 0.05$ was regarded as indicative of a significant difference.

Classification of tumor samples based on the total TMB score

The TMB is a measure of the total number of mutations per megabyte of DNA in tumor tissue. We calculated the TMB using the "maftools" R package (version 2.2) [20,37]. A waterfall plot was constructed to visualize the top 20 genes that were most frequently mutated in the two groups. The co-occurrence and mutual exclusion of mutated genes were calculated in the two groups.

Functional analysis

The Wilcoxon test was used to detect the differences in gene expression between two groups with the "limma" R package (version 3.4). The cutoff values to define the differentially expressed genes (DEGs) were log (fold change (FC)) > 0.5 and false discovery rate (FDR) < 0.05. For enrichment map, a ranked list of the DEGs was used to generate enrichment scores using the GSEA Preranked module of GSEA (v3.0). Given the symmetrical nature of the ranked list, the weighted statistic was applied. Hallmark and C2: Canonical Pathway gene sets were downloaded from the MSigDB database (v6.2) (http://software.broadinstitute.org/gsea/msigdb/genesets.jsp).

Estimation of intratumoral infiltrated immune cells

Three methods were used to estimate the fractions of immune cells in

the TME. First, we used the CIBERSORT algorithm to calculate the expression of markers of 22 immune cell types and their compositions of patients in TCGA. Second, ssGSEA was conducted to calculate the expression levels of 29 immunity-associated signatures using the 'GSVA' package (v1.30.0). Third, we estimated the proportions of infiltrated immune cells with Tumor Immune Estimation Resource (TIMER) 2.0 (https://cistrome.shinyapps.io/timer/), where seven algorithms, comprising TIMER, EPIC, CIBERSORT, quanTIseq, xCell, MCP-counter and TIDE, were applied in the analysis [38]. The quantitative correlation between the adipocyte IS and immune checkpoints was evaluated by calculating the Pearson correlation coefficient (r).

IHC staining

Clinical tissue samples used in this study for IHC were obtained from patients diagnosed with PDAC at FUSCC. Prior patient consent and approval from the Institutional Research Ethics Committee were obtained. IHC staining of paraffin-embedded tissues with antibodies against FABP4 and CD8 was performed to detect FABP4 and CD8-positive cells using standard procedures [39]. The anti-FABP4 antibody (12802-1-AP, Proteintech) was used at a dilution of 1:100, and the anti-CD8 antibody (66868-1-Ig, Proteintech) was used at a dilution of 1:4000.

Quantitative real-time PCR (qRT-PCR)

Sixty-eight paired PDAC samples were collected from histopathologically and clinically diagnosed patients at the FUSCC. The expression levels of candidate genes were determined using the SYBR® Green Premix Pro Taq HS qPCR Kit (Rox Plus) AG11718. The primer sequences for FABP4 used in this study were as follows: forward primer, ACTGGGCCAGGAATTTGACG; and reverse primer, CTCGTGGAAGTGACGCCTT.

Cell culture

The Pan02 cell line was purchased from the National Infrastructure of Cell Line Resources. Cells were cultured in Dulbecco's modified Eagle's medium (DMEM) supplemented with 10% fetal bovine serum (FBS), 100 units/mL penicillin, and 100 μg/mL streptomycin.

Animal studies

Six-week-old female nude mice and C57BL/6J mice were obtained from Shanghai SLAC Laboratory. All mice were housed and maintained under specific pathogen-free conditions and used in accordance with institutional guidelines. These mice were randomly divided into three subgroups (n=4 mice/group). Pan02 cells and adipocytes were subcutaneously inoculated into the left flanks of the mice. We determined the tumor size twice a week after the formation of palpable tumors and calculated the tumor volume using the following formula: length × width [2] × 0.5. At 3 weeks post-implantation, the tumor specimens were surgically dissected and digested for analysis with flow cytometry or fixed with paraformaldehyde and then subjected to IHC staining. The protocol was approved by the Committee on the Ethics of Animal Experiments of FUSCC.

Statistics

The data were analyzed using SPSS software (V.21.0; IBM Corporation), GraphPad Prism (V.8.3; California, USA) or R (V.4.1.0). The cumulative survival time was analyzed using the Kaplan–Meier method and log-rank test. Student's t test or ANOVA was used for comparisons between groups. All statistical analyses were 2-sided, and P values < 0.05 were considered statistically significant. $^{*}P < 0.05$, $^{**}P < 0.01$, and $^{***}P < 0.001$.

Authors' contributions

XL and JL performed the bioinformatics analyses; JX performed the statistical analyses; BZ, MW, JL, HX and XY checked the tables and figures; and WW and SS designed the study. All authors read and approved the final manuscript.

Ethical approval and consent to participate

The clinical tissue samples used in this study were obtained from patients diagnosed with pancreatic cancer at FUSCC. Prior patient consent and approval from the Institutional Research Ethics Committee were obtained. All animal experiments were approved by the Committee on the Ethics of Animal Experiments of FUSCC.

Declaration of Competing Interest

The authors have no conflicts of interest to declare.

Acknowledgments

We thank the editors at AJE (American Journal Experts) for their assistance with editing the manuscript, and all conceptual graphs were created with BioRender.com. This study was jointly supported by grants from the National Natural Science Foundation of China (U21A20374), Shanghai Municipal Science and Technology Major Project (21JC1401500), Scientific Innovation Project of Shanghai Education Committee (2019-01-07-00-07-E00057), Clinical Research Plan of Shanghai Hospital Development Center (SHDC2020CR1006A), and Xuhui District Artificial Intelligence Medical Hospital Cooperation Project (2021-011).

Supplementary materials

Supplementary material associated with this article can be found, in the online version, at doi:10.1016/j.tranon.2022.101561.

References

[1] H. Sung, J. Ferlay, R.L. Siegel, M. Laversanne, I. Soerjomataram, A. Jemal, F. Bray, Global cancer statistics 2020: GLOBOCAN estimates of incidence and mortality worldwide for 36 cancers in 185 countries, CA Cancer J. Clin. 71 (2021) 209–249.
[2] J.D. Mizrahi, R. Surana, J.W. Valle, RT. Shroff, Pancreatic cancer, Lancet 395 (2020) 2008–2020.
[3] I. Garrido-Laguna, M. Hidalgo, Pancreatic cancer: from state-of-the-art treatments to promising novel therapies, Nat. Rev. Clin. Oncol. 12 (2015) 319–334.
[4] T. Conroy, P. Hammel, M. Hebbar, FOLFIRINOX or gemcitabine as adjuvant therapy for pancreatic cancer, N. Engl. J. Med. 379 (2018) 2395–2406.
[5] A.S. Bear, R.H. Vonderheide, M.H. O'Hara, Challenges and opportunities for pancreatic cancer immunotherapy, Cancer Cell 38 (2020) 788–802.
[6] W.J. Ho, E.M. Jaffee, L. Zheng, The tumour microenvironment in pancreatic cancer - clinical challenges and opportunities, Nat. Rev. Clin. Oncol. 17 (2020) 527–540.
[7] M. Binnewies, E.W. Roberts, K. Kersten, Understanding the tumor immune microenvironment (TIME) for effective therapy, Nat. Med. 24 (2018) 541–550.
[8] X. Liu, J. Xu, B. Zhang, J. Liu, C. Liang, Q. Meng, J. Hua, X. Yu, S. Shi, The reciprocal regulation between host tissue and immune cells in pancreatic ductal adenocarcinoma: new insights and therapeutic implications, Mol. Cancer 18 (2019) 184.
[9] K.G. Anderson, I.M. Stromnes, PD. Greenberg, Obstacles posed by the tumor microenvironment to t cell activity: a case for synergistic therapies, Cancer Cell 31 (2017) 311–325.
[10] H. Sung, R.L. Siegel, L.A. Torre, J. Pearson-Stuttard, F. Islami, S.A. Fedewa, A. Goding Sauer, K. Shuval, S.M. Gapstur, E.J. Jacobs, et al., Global patterns in excess body weight and the associated cancer burden, CA Cancer J. Clin. 69 (2019) 88–112.
[11] B. Lauby-Secretan, C. Scoccianti, D. Loomis, Y. Grosse, F. Bianchini, K. Straif, Body fatness and cancer–viewpoint of the IARC working group, N. Engl. J. Med. 375 (2016) 794–798.
[12] B.M. Wolpin, Y. Bao, Z.R. Qian, C. Wu, P. Kraft, S. Ogino, M.J. Stampfer, K. Sato, J. Ma, J.E. Buring, et al., Hyperglycemia, insulin resistance, impaired pancreatic β-cell function, and risk of pancreatic cancer, J. Natl. Cancer Inst. 105 (2013) 1027–1035.
[13] R. Carreras-Torres, M. Johansson, V. Gaborieau, P.C. Haycock, K.H. Wade, C. L. Relton, R.M. Martin, G. Davey Smith, P. Brennan, The role of obesity, type 2

diabetes, and metabolic factors in pancreatic cancer: a mendelian randomization study, J. Natl. Cancer Inst. 109 (9) (2017) djx012.
[14] N. Murphy, M. Jenab, MJ. Gunter, Adiposity and gastrointestinal cancers: epidemiology, mechanisms and future directions, Nat. Rev. Gastroenterol. Hepatol. 15 (2018) 659–670.
[15] E. Lengyel, L. Makowski, J. DiGiovanni, MG. Kolonin, Cancer as a matter of fat: the crosstalk between adipose tissue and tumors, Trends Cancer 4 (2018) 374–384.
[16] T. Deng, C.J. Lyon, S. Bergin, M.A. Caligiuri, WA. Hsueh, Obesity, inflammation, and cancer, Annu. Rev. Pathol. 11 (2016) 421–449.
[17] J. O'Sullivan, J. Lysaght, C.L. Donohoe, JV. Reynolds, Obesity and gastrointestinal cancer: the interrelationship of adipose and tumour microenvironments, Nat. Rev. Gastroenterol. Hepatol. 15 (2018) 699–714.
[18] S. Guaita-Esteruelas, J. Gumà, L. Masana, J. Borràs, The peritumoural adipose tissue microenvironment and cancer. The roles of fatty acid binding protein 4 and fatty acid binding protein 5, Mol. Cell. Endocrinol. 462 (2018) 107–118.
[19] B. Dirat, L. Bochet, M. Dabek, D. Daviaud, S. Dauvillier, B. Majed, Y.Y. Wang, A. Meulle, B. Salles, S. Le Gonidec, et al., Cancer-associated adipocytes exhibit an activated phenotype and contribute to breast cancer invasion, Cancer Res. 71 (2011) 2455–2465.
[20] R. Tang, X. Liu, W. Wang, J. Hua, J. Xu, C. Liang, Q. Meng, J. Liu, B. Zhang, X. Yu, et al., Role of tumor mutation burden-related signatures in the prognosis and immune microenvironment of pancreatic ductal adenocarcinoma, Cancer Cell Int. 21 (2021) 196.
[21] N. Nisha, W.M. S, Z. Weiping, Chemokines in the cancer microenvironment and their relevance in cancer immunotherapy, Nat. Rev. Immunol. 17 (9) (2017) 559–572.
[22] M. Kyrgiou, I. Kalliala, G. Markozannes, M.J. Gunter, E. Paraskevaidis, H. Gabra, P. Martin-Hirsch, KK. Tsilidis, Adiposity and cancer at major anatomical sites: umbrella review of the literature, BMJ 356 (2017) j477.
[23] World Cancer Research Fund/American Institute for Cancer Research. (2007). Food, nutrition, physical activity, and the prevention of pancreatic cancer. https://discovery.ucl.ac.uk/id/eprint.
[24] A. Neesse, C.A. Bauer, D. Öhlund, M. Lauth, M. Buchholz, P. Michl, D.A. Tuveson, TM. Gress, Stromal biology and therapy in pancreatic cancer: ready for clinical translation? Gut 68 (2019) 159–171.
[25] Cancer Genome Atlas Research Network, Integrated genomic characterization of pancreatic ductal adenocarcinoma, Cancer Cell. 32 (2) (2017) 185–203.
[26] G. Eibl, E. Rozengurt, KRAS, YAP, and obesity in pancreatic cancer: a signaling network with multiple loops, Semin. Cancer Biol. 54 (2019) 50–62.
[27] A. Stenzinger, J.D. Allen, J. Maas, M.D. Stewart, D.M. Merino, M.M. Wempe, M. Dietel, Tumor mutational burden standardization initiatives: Recommendations for consistent tumor mutational burden assessment in clinical samples to guide immunotherapy treatment decisions, Genes Chromosomes Cancer 58 (8) (2019) 578–588.
[28] B. Cabia, S. Andrade, M.C. Carreira, F.F. Casanueva, AB. Crujeiras, A role for novel adipose tissue-secreted factors in obesity-related carcinogenesis, Obes. Rev. 17 (2016) 361–376.
[29] G. Maurizi, L. Della Guardia, A. Maurizi, A. Poloni, Adipocytes properties and crosstalk with immune system in obesity-related inflammation, J. Cell. Physiol. 233 (2018) 88–97.
[30] G. Donninelli, M. Del Cornò, M. Pierdominici, B. Scazzocchio, R. Varì, B. Varano, I. Pacella, S. Piconese, V. Barnaba, M. D'Archivio, et al., Distinct blood and visceral adipose tissue regulatory T cell and innate lymphocyte profiles characterize obesity and colorectal cancer, Front. Immunol. 8 (2017) 643.
[31] T. Pecht, A. Gutman-Tirosh, N. Bashan, A. Rudich, Peripheral blood leucocyte subclasses as potential biomarkers of adipose tissue inflammation and obesity subphenotypes in humans, Obes. Rev. 15 (2014) 322–337.
[32] W.J. Ho, E.M. Jaffee, L. Zheng, The tumour microenvironment in pancreatic cancer - clinical challenges and opportunities, Nat. Rev. Clin. Oncol. 17 (2020) 527–540.
[33] H. Lee, J. Palm, S.M. Grimes, H.P. Ji, The cancer genome atlas clinical explorer: a web and mobile interface for identifying clinical-genomic driver associations, Genome Med 7 (2015) 112.
[34] D.A. Barbie, P. Tamayo, J.S. Boehm, S.Y. Kim, S.E. Moody, I.F. Dunn, A.C. Schinzel, P. Sandy, E. Meylan, C. Scholl, et al., Systematic RNA interference reveals that oncogenic KRAS-driven cancers require TBK1, Nature 462 (2009) 108–112.
[35] D. Aran, Z. Hu, AJ. Butte, xCell: digitally portraying the tissue cellular heterogeneity landscape, Genome Biol. 18 (2017) 220.
[36] X. Zhang, Y. Lan, J. Xu, F. Quan, E. Zhao, C. Deng, T. Luo, L. Xu, G. Liao, M. Yan, et al., CellMarker: a manually curated resource of cell markers in human and mouse, Nucleic Acids Res. 47 (2019) D721–D728.
[37] S. Hänzelmann, R. Castelo, J. Guinney, GSVA: gene set variation analysis for microarray and RNA-seq data, BMC Bioinform. 14 (2013) 7.
[38] T. Li, J. Fu, Z. Zeng, D. Cohen, J. Li, Q. Chen, B. Li, S. Liu, TIMER2.0 for analysis of tumor-infiltrating immune cells, Nucleic Acids Res. 48 (2020) W509–W514.
[39] C. Liang, S. Shi, Y. Qin, Q. Meng, J. Hua, Q. Hu, S. Ji, B. Zhang, J. Xu, X.J. Yu, Localisation of PGK1 determines metabolic phenotype to balance metastasis and proliferation in patients with SMAD4-negative pancreatic cancer, Gut 69 (5) (2020) 888–900.